

**INFORMATION SUPPLIED BY K. DOBROLYUBOVA (Aug 2011)**

**I. SOME REFERENCES FOR THE “BELLINGSHAUSEN BASIN” UFN**

G.Schott, 1935. Geographie des Indiscen und Stillen ozeans, Verlag: C.Boysen, Hamburg.

Marine Atlas. 1950 r. Pub. USSR Navy Ministry.

ARNOLD L. GORDON. **Potential temperature, oxygen and circulation of bottom water in the Southern Ocean** (Received 10 May 1966)./ Deep-Sea Research, 1966, Vol. 13, pp. 1125 to 1138. Pergamon Press Ltd. Printed in Great Britain

**Papers from**

**Initial Reports of the Deep Sea Drilling Project. Volume XXXV**  
covering Leg 35 of the cruises of the Drilling vessel *Glomar Challenger*  
Callao, Peru to Ushuaia, Argentina February-March 1974

**PARTICIPATING SCIENTISTS**

Charles D. Hollister, Campbell Craddock, Yury A. Bogdanov,  
N. Terence Edgar, Joris M. Gieskes, Bilal U. Haq, James R. Lawrence,  
Fred Rögl, Hans-Joachim Schrader, Brian E. Tucholke,  
Walter R. Vennum, Fred M. Weaver, Vasily N. Zhivago

SCIENCE EDITOR

Paula Worstell

Prepared for the NATIONAL SCIENCE FOUNDATION

National Ocean Sediment Coring Program

Under Contract C-482

By the UNIVERSITY OF CALIFORNIA

Scripps Institution of Oceanography

Prime Contractor for the Project

**7. SEDIMENTARY FRAMEWORK OF THE BELLINGSHAUSEN BASIN  
FROM SEISMIC PROFILER DATA1**

Brian E. Tucholke and Robert E. Houtz,  
Lamont-Doherty Geological Observatory of Columbia University, Palisades, New York  
[http://www.deepseadrilling.org/35/volume/dsdp35\\_07.pdf](http://www.deepseadrilling.org/35/volume/dsdp35_07.pdf)

**9. A GEOPHYSICAL SURVEY AT SITE 325 IN THE BELLINGSHAUSEN BASIN1**

Fred W. Schroeder,2 Lamont-Doherty Geological Observatory of Columbia University, Palisades, New York  
[http://www.deepseadrilling.org/35/volume/dsdp35\\_09.pdf](http://www.deepseadrilling.org/35/volume/dsdp35_09.pdf)

Atlas of the Oceans. Pacific ocean. 1974. Pub. USSR Ministry of Defence.

Lynne D. Talley and Mizuki Tsuchiya, Scripps Institution of Oceanography/UCSD, La Jolla, CA 92093-0230, USA  
WOCE P19 in the Eastern South Pacific.

International WOCE Newsletter, N 19, June 1995

**International Geological-Geophysical Atlas of the Pacific Ocean.**

Published in accordance with the decision of the Intergovernmental Oceanographic Commission. Editorial board: G. Udintsev(ch.ed.), D.Scott, I.Gramberg, B.T.R.Lewis, K.Seichiro, M.Talwani, S.Ueda (principal scientific advisor).  
p. 44

## II. WOCE P19 in the Eastern South Pacific

*Lynne D. Talley and Mizuki Tsuchiya, Scripps Institution of Oceanography/UCSD, La Jolla, CA 92093-0230, USA*

### Cruise summary

WHP section P19C along 88° E was carried out on RV Knorr between Punta Arenas, Chile, and Panama City, Panama, from 22 February to 13 April 1993. P19C was the seventh Pacific WOCE hydrographic leg on the Knorr and the fourth with basic technical support from Scripps Institution of Oceanography's Oceanographic Data Facility (SIO/ODF). The cruise track (Fig. 1) was east of the East Pacific Rise for its entire length, and crossed four deep basins (Bellingshausen, Chile, Panama and Guatemala) separated by ridges (Sala y Gomez, Carnegie and Cocos). The track went westward along 54° S out to 88° W and then northward along 88°W and 85°50'W, up to 4°N where the track turned northwestward and then into Central America off Guatemala. This first section is an abbreviated version of the cruise report which was filed with the WOCE Hydrographic Programme Office. The complete cruise report can be obtained from the WHPO at WHOI or through anonymous ftp to sam.ucsd.edu in subdirectory pub/p19 which also includes postscript files for some of the basic

vertical sections. Section 2 is a very brief description of some hydrographic features found along the section.

All stations were to within 10 metres of the bottom and included a rosette/CTD cast. Basic station spacing was 30 nm, closing to 20 nm for 3° S – 1° S and 1° N – 3° N, and to 10 nm for 1° S to 1° N. Station spacing at the Chilean and Guatemalan coasts and over the Sala y Gomez Ridge (about 25° S) was less than 30 nm and dictated by topography. Sampling included 108 CTD/rosette stations, 13 large volume sampling (Gerard barrel) stations, and 20 200-metre bio-optics stations (J. Marra of LDEO for JGOFS). Sampling was done with a 36-place General Oceanics pylon on a rosette frame with 10-litre bottles and a CTD, transmissometer, altimeter and pinger. An RDI lowered acoustic doppler profiler (Eric Firing) was mounted inside the rosette frame for 94 stations.

The CTD data stream consisted of elapsed time, pressure, two temperature channels, conductivity, oxygen, altimeter and transmissometer signals. There were no major problems with the CTD measurements. Most of the few problems in conductivity resulted from biological

fouling of the rosette/CTD during the cast.

Water samples were collected for analyses of salt, oxygen, silica, phosphate, nitrate and nitrite on all stations and of CFC-11, CFC-12, helium-3, helium-4, tritium, AMS  $^{14}\text{C}$ ,  $\text{pCO}_2$ , and total dissolved inorganic carbon on selected stations.

Discrete salinity, oxygen and nutrient values were compared with preliminary data acquired on P17E (Swift, chief scientist, RV Knorr) and P6 (Bryden, chief scientist, RV Knorr), and with data from the 1989 Moana Wave cruise at  $9^\circ 30'\text{N}$  and the two old 1968 Scorpio sections at  $43^\circ \text{S}$  and  $28^\circ \text{S}$ . A complete version of the comparisons, with figures and tables, can be found in the WHP P19C cruise report available from anonymous ftp. Salinity accuracy is within WOCE requirements on P19C and the

*volume plus rosette/CTD station (crossed circles).*

*International WOCE Newsletter, Number 19, March 1995*

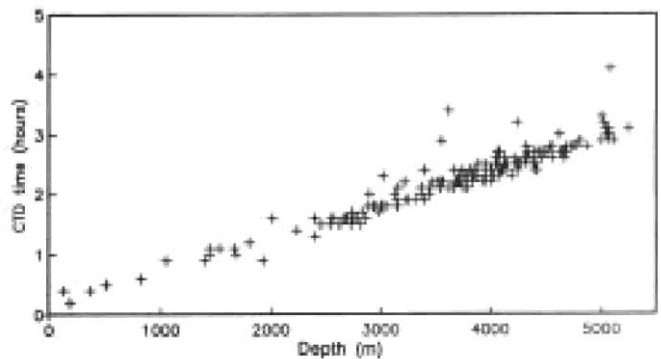
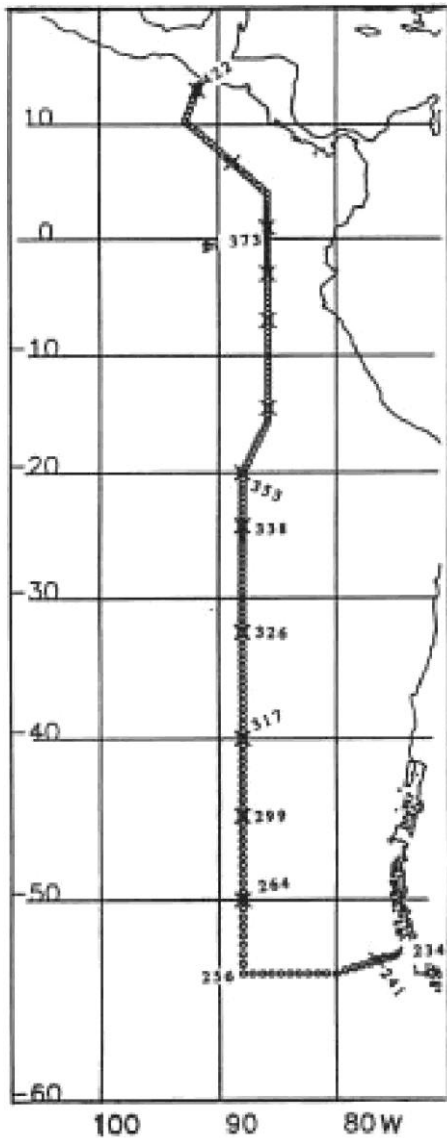


*Figure 1. Cruise track for WOCE P19C (RV Knorr 138-12), 22 February 1993 – 13 April 1993. Rosette/CTD stations (circles). Large*

other recent cruises. There are offsets in oxygen amongst the recent cruises which are larger than the precision required but within the accuracy limits, so indicating no fundamental problems. In nutrients however, there may be inter-group differences which exceed the WHP requirements for accuracy.

CTD/rosette station times are shown in Fig. 2. These times are comparable to those from two previous Knorr WOCE legs. These numbers do not include start and stop times, so actual stations times were about 5 minutes longer. Wire speeds were generally 60 metres/minute for downcasts and 70 metres/minute for upcasts; because of stops for bottle trips and slower speeds in the upper 200 metres, the average wire speed for all stations was 55–58 metres/ minute.

Towards the end of the cruise, we started to wait for a few ship rolls before closing bottles in the strong near-surface pycnocline in order to flush the bottle, as suggested long ago by Ray Weiss of SIO. This reduced the differences in CTD and bottle conductivity by two to three orders of magnitude. This suggests that the concept of closing bottles “on the fly” may result in degradation of CTD calibration, particularly in the pycnocline.

Large-volume sampling (R. Key of Princeton) was made with use of 270-litre Gerard barrels for analyses of  $^{14}\text{C}$ , salinity, oxygen and nutrients on 13 stations. All covered the water column below 1000 metres.  $^{14}\text{C}$  samples were collected from the rosette for the upper 1000 metres for analysis by AMS.

Underway measurements included Acoustic Doppler Current Profiling (Eric Firing of U. Hawaii),  $\text{pCO}_2$ ,  $\text{pN}_2\text{O}$  (R. Weiss, SIO), and the various variables of Knorr’s IMET system (surface water temperature and conductivity, oxygen, meteorological parameters, GPS navigation, ship’s speed and heading). Underway bathymetry was recorded every 5 minutes from the Knorr’s PDR for our own use in constructing vertical sections and as additional input to the overall data-base (S. Smith - Geological Data Center at SIO).

Twenty-one subsurface ALACE floats were deployed for R. Davis of SIO. The ballast pressure for the floats was 800 to 850 dbar. Six surface drifters were deployed for P. Niiler of SIO.

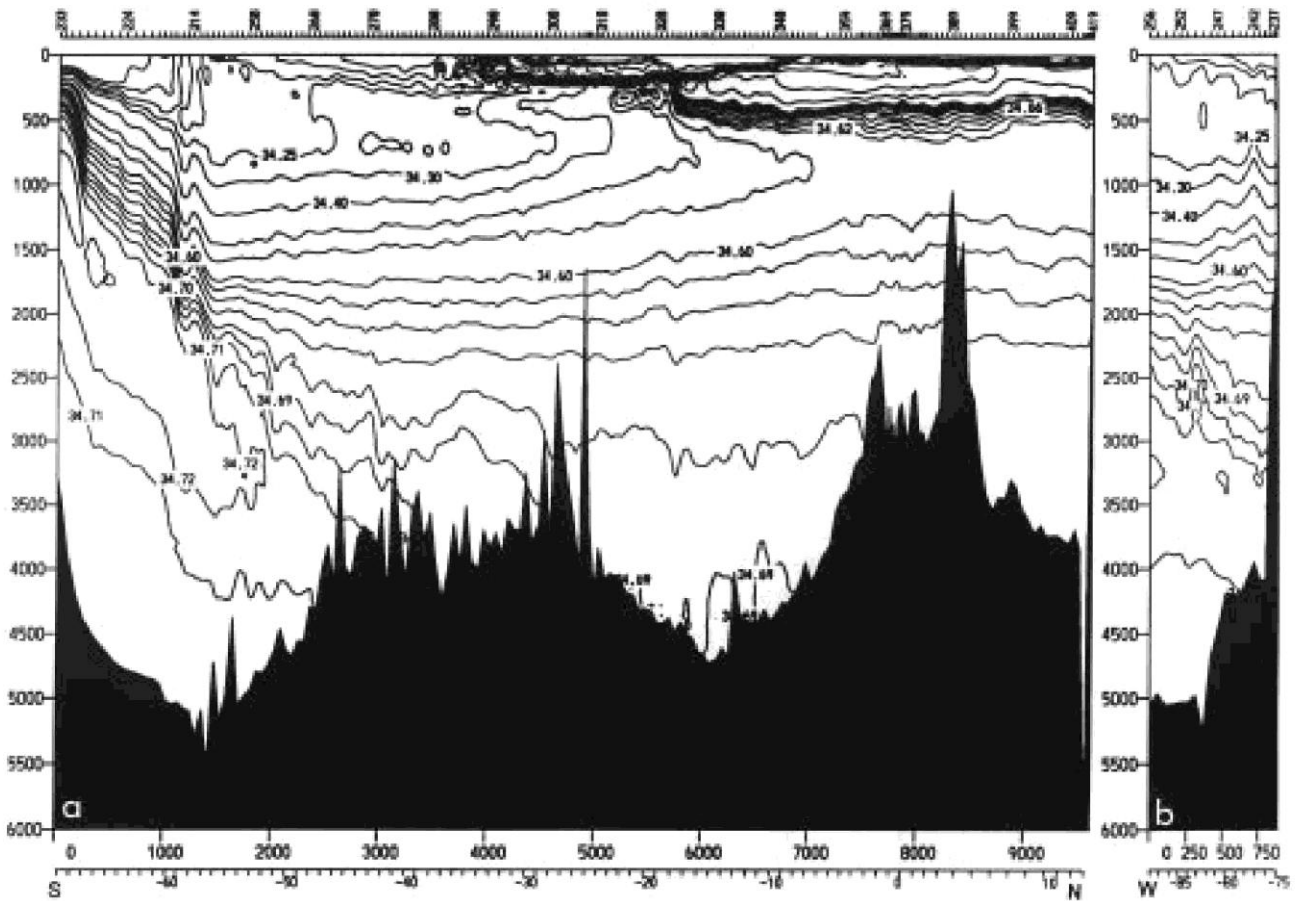


Figure 3. Vertical section of salinity along (a) 88°W and (b) 54°S from 88°W to South America. The portion of 88°W south of 54°S was collected by J. Swift of SIO on the previous WOCE leg on the RV Knorr.

Preliminary results

Vertical sections of potential temperature, salinity, oxygen and silica illustrate some of the major water mass features encountered along 88° W and eastward along 54° S. The 88° W section was extended southwards in Figs. 3 and 4 with the stations collected on the preceding leg by Swift (see article in International WOCE Newsletter No. 18), which are used here with his permission.

1. The major Pacific water masses on the section were Antarctic Intermediate Water (stability and salinity minimum/oxygen maximum at 400–600 metres), Pacific Deep Water (oxygen minimum at 1500–2000 metres and silica maximum at about 2800 metres),

North Atlantic Deep Water or Upper Circumpolar Water (salinity maximum at about 3500 metres), and Antarctic Bottom Water or Lower Circumpolar Water (oxygen maximum and salinity minimum at the bottom). At the top of the Chile Rise, between 43° and 41° S, the Antarctic Bottom Water and Circumpolar Water disappeared and did not reappear as we crossed into the western portion of the Chile Basin. The Chile Basin was filled to the bottom with a much more homogeneous water mass than in the Bellingshausen Basin, with high silica, low oxygen and relatively

warm water (greater than 1.4° C). The sill depth for the Chile Basin appears to be at about 3500 m. The bottommost waters in the Chile Basin have higher oxygen and lower silica than those above, indicating southern origin.

2. At 54° S off the coast of Chile there was a clear eastern boundary regime of about 500 km width at 54° S, extending to the ocean bottom. Characteristics of this regime are relatively low oxygen in the Pacific Deep Water oxygen minimum, relatively low salinity in the Circumpolar Water salinity maximum, relatively high silica in the Pacific Deep Water silica maximum, and potential vorticity signatures for these

water masses which also indicate an eastern boundary regime. Properties in this eastern boundary region match fairly well with those found at the northern side of the Bellingshausen Basin, between about 45 and 50° S. Large-scale currents are therefore probably southward to the bottom along the eastern boundary, out to 81° W. They are also eastward along 88° W at the northern side of the Bellingshausen Basin, indicating cyclonic flow in accord with Reid (1986).

3. The near-surface waters in a large patch west of southern Chile (54° S, 79° W up to 52° S, 88° W) were very similar to Antarctic Intermediate Water (AAIW).

The salinity minimum was nearly non-existent in this outcrop region and the oxygen in the pycnostad was at the surface value. The density of the thick pycnostad was  $27.01 \text{ s}_\sigma$ . This was only slightly less dense than the well-defined salinity minimum AAIW found east and north of the patch ( $27.02 \text{ s}_\sigma$ ). A well-defined oxygen maximum was also found in the AAIW east and north of the patch. Dynamic height at the surface relative to deeper levels was essentially flat throughout the patch, rising both to the east and to the north, suggesting a broad cyclonic flow around it of waters which then enter Drake Passage. This suggests that the local Subantarctic Mode Water in the southeastern Pacific is essentially identical to the AAIW which spreads northward, probably by subduction, in the eastern South Pacific.

The low potential vorticity signature of the AAIW was found as far north as about  $30^\circ \text{ S}$ . The well-defined oxygen maximum associated with the AAIW is found as far north as about  $24^\circ \text{ S}$ . The salinity minimum of course extends to the northern end of the section in the North Pacific off Guatemala. The density of the salinity minimum shifts rapidly from about  $27.1 \text{ s}_\sigma$  to  $27.3 \text{ s}_\sigma$  between  $20^\circ$  and  $17^\circ \text{ S}$ . There is significant fine structure (interleaving) at the

minimum between about  $23^\circ \text{ S}$  and  $17^\circ \text{ S}$ . The highest salinity AAIW is found in the equatorial region and north of the equator. Oxygen in the equatorial AAIW is  $0.5 \text{ ml/l}$  higher than under the low oxygen regimes  $10^\circ$  south and  $5^\circ$  north of the equator.

4. Low salinity surface water extending westward from South America centred at about  $40^\circ \text{ S}$  was evident in prior work, and has been called the Deacon jet. This fresh water was very clearly defined along  $88^\circ \text{ W}$  between  $54^\circ \text{ S}$  and  $34^\circ \text{ S}$ , with an abrupt front at the northern edge. Changes in dynamic height at the surface relative to deeper levels suggest eastward flow throughout the low salinity tongue, despite the apparent source of the lowest salinity water to the east, based on historical data. It extends down to about 200 metres and is the apparent source of the shallow salinity minimum found in the northern subtropical gyre of the South Pacific. The shallow salinity minimum is evident on this section between  $38^\circ \text{ S}$  and  $20^\circ \text{ S}$ .
5. There was an isopycnal uplift at station 242, at  $54^\circ \text{ S}$ ,  $77^\circ \text{ W}$ , in the upper 1500 metres, accompanied by even stronger uplift of properties. This suggests a cyclonic flow around the rise offshore of the Chile Trench.

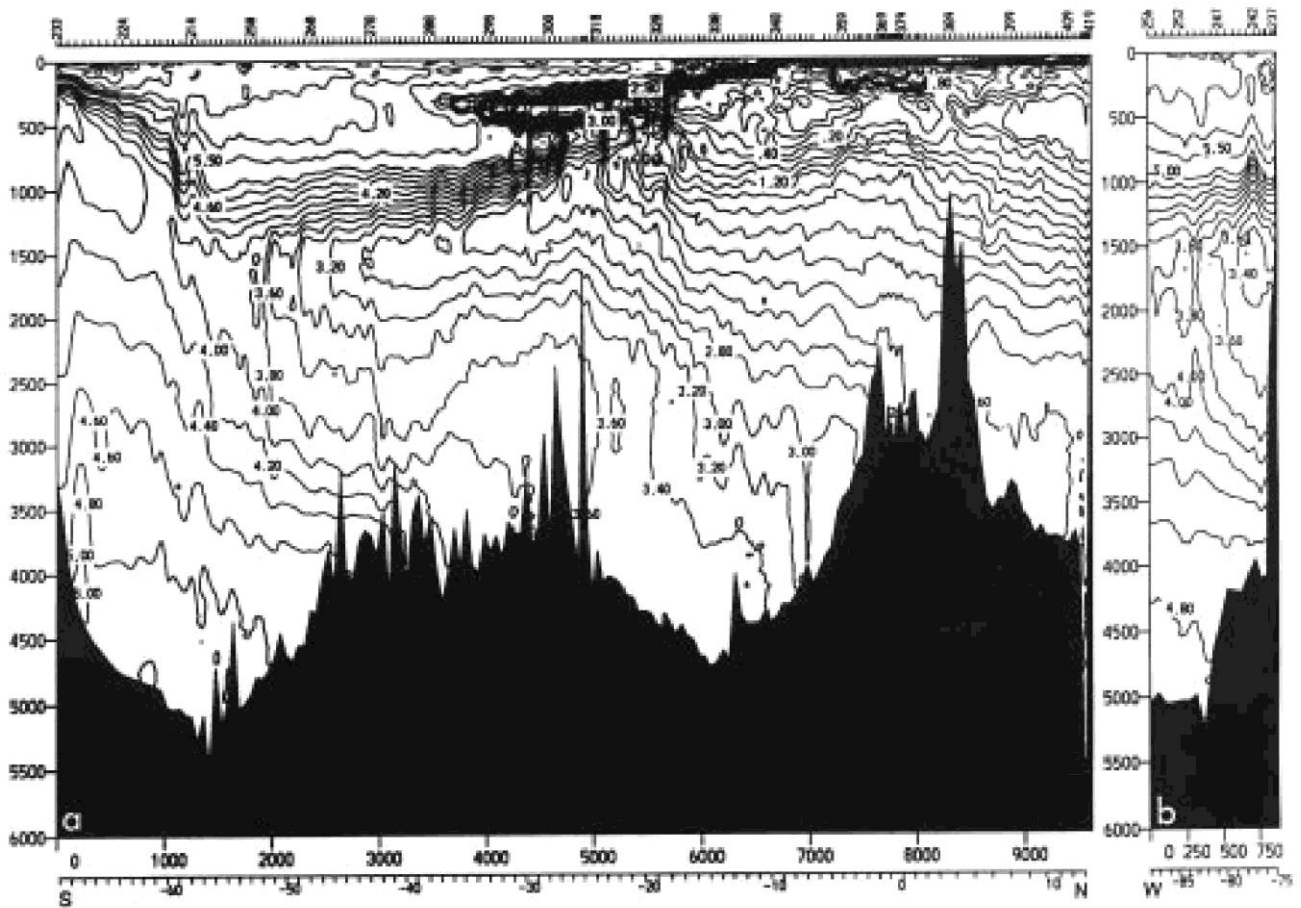


Figure 4. Vertical section of oxygen (ml/l) along (a) 88°W and (b) 54°S from 88°W to South America.



6. The high salinity northern subtropical surface water penetrates to about 200 metres depth between its onset near 38° S up to about 20° S (northern limit of the underlying salinity minimum). North of this, the higher salinity influence plunges down to about 500 metres, and north of about 12° S there is a well-defined subsurface salinity maximum at about 100 metres depth.
7. The section crossed the equator in the deepest part of the narrow region between the Galapagos Islands and South America. The maximum depth here was around 3000 metres. This is an active geothermal region. Centred about the equator the bottom water was noticeably warmer (by 0.3° C) than on either side of the bathymetric rise, and quite uniform over about 700 metres from the bottom. This uniform bottom layer was also more uniform in oxygen and salinity than on either side of the equator, indicating mixing. The equatorial band (within 2° of the equator) also has striking vertical structure from 500 metres to the

ocean bottom, evidenced in an increase in layering as quantified by minima and maxima of Vaisala frequency, compared with the more monotonic structure farther from the equator. 8. The oxygen minima north and south of the equator in this region are notable for the very low values of oxygen very close to the surface (less than 0.02 ml/l). The oxycline separating the surface saturated layer from the underlying minimum layer lies at about 50 metres depth. A double nitrite maximum is found associated with the oxygen minima north and south of the equator: south of the equator the deeper nitrite maximum is at about 150 metres and north of the equator it is centred at 400 metres.

### Reference

- Reid, J.L., 1986: On the total geostrophic circulation of the South Pacific Ocean: flow patterns, tracers and transports. *Prog. Oceanogr.*, 16: 1-61.

## WOCE Observations in the Pacific Ocean

*N.P. Holliday, WOCE IPO*

During the years 1991–1994 the Pacific Ocean was subjected to an intensive one-time survey resulting in the grid of sections illustrated in Fig. 1. Repeated hydrographic sections, time series stations, current meter moorings and high density XBT sections began in 1990 and will continue to monitor the Pacific through 1997. Fig. 2 shows schematically where the continuing observations are. Absent from Fig. 2 are the low density XBT sections, subsurface floats, surface drifting buoys and sea level stations which will also continue throughout the WOCE Field Phase.

Providing WOCE data and products to a large science community in a timely way is a



central aim of WOCE, in order that the data

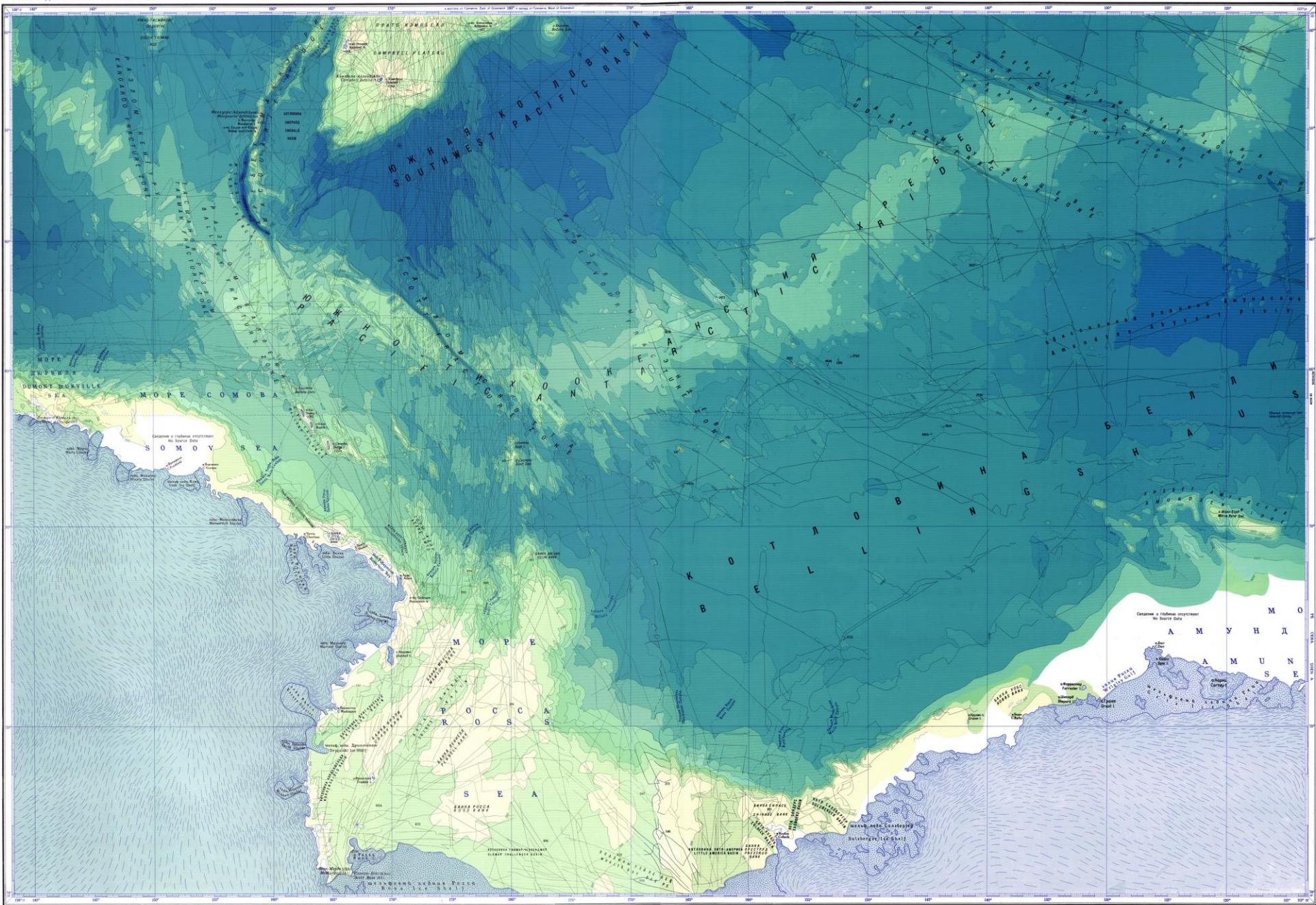
from individual sections and projects can be included in the wider synthesis of WOCE data. Many of the data sets collected since 1990 should now be in the public domain but still

*Figure 1. Completed Pacific Ocean One Time Survey Sections.*



**МЕЖДУНАРОДНЫЙ  
ГЕОЛОГО-ГЕОФИЗИЧЕСКИЙ  
АТЛАС  
ТИХОГО ОКЕАНА**

**INTERNATIONAL  
GEOLOGICAL-GEOPHYSICAL  
ATLAS OF THE  
PACIFIC OCEAN**

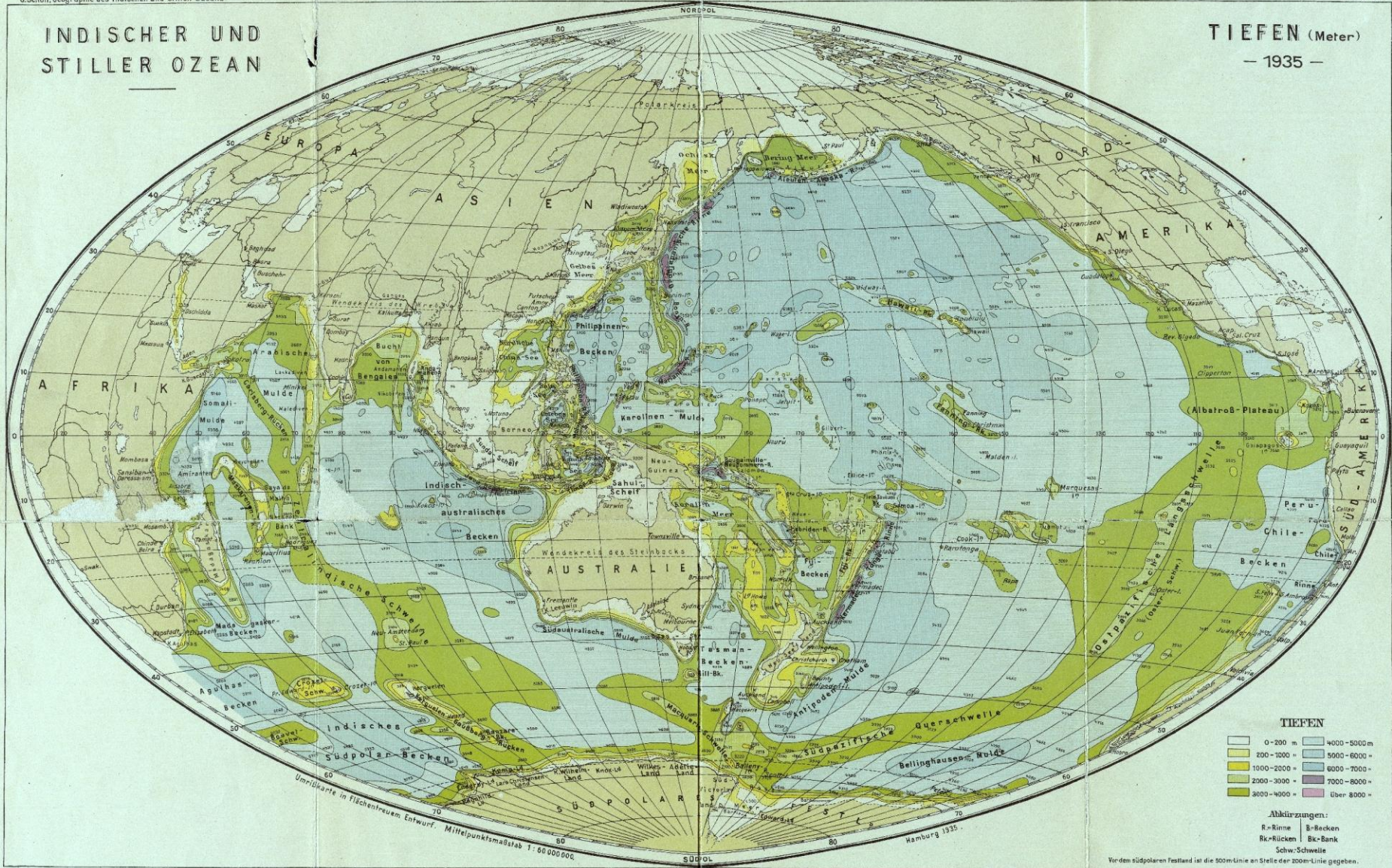


Масштаб 1:10 000 000 по параллели 40°  
Scale 1:10,000,000 at latitude 40°



# INDISCHER UND STILLER OZEAN

# TIEFEN (Meter) — 1935 —



**TIEFEN**

0-200 m	4000-5000 m
200-1000 m	5000-6000 m
1000-2000 m	6000-7000 m
2000-3000 m	7000-8000 m
3000-4000 m	Über 8000 m

**Abkürzungen:**  
 R-Rinne | B-Becken  
 Rk-Rücken | Bk-Bank  
 Schw-Schwelle

Wirdem südpolaren Festland bei der 500m-Linie an Stelle der 200m-Linie gegeben.

## Potential temperature, oxygen and circulation of bottom water in the Southern Ocean\*

ARNOLD L. GORDON!

{Received 10 May 1966}

Abstract—The circulation of bottom and near-bottom water can be determined in a qualitative manner by inspecting parameter distributions. Bottom potential temperature and oxygen (which show a definite relation in the *tp-Ov* diagram) are very useful for this purpose in the portion of the Southern Ocean dealt with in this paper (20°W westward to 170°W and south of 50°S). Observations used are deeper than 3000 m and within 300 m of the bottom.

There are two areas of cold water (< 0-0°C): the more extreme emanating from the Weddell Sea and the other from the Ross Sea. The Weddell Sea Bottom Water flows to the east of the South Sandwich Trench into the Argentine Basin, though some water does enter the trench and flows northward. The bottom waters of the Scotia Sea come from between the 3000-3200 m level of the Weddell Sea through a passage at 39°W in the South Orkney Ridge. A tongue of this water flows into the southern Drake Passage, confining to the northern Drake Passage the warmer bottom water from the Pacific Ocean. This warmer bottom water forms a rapid easterly current which enters the South Atlantic west of Shag Rocks. The cold Scotia Sea bottom water does not penetrate the Pacific Ocean but is topographically or dynamically restrained. Circulation in the eastern Scotia Sea is weak to moderate.

A cold-water tongue in the **Bellingshausen Basin** is bounded by a band of warm water on its north-west and northeast sides. It is probable that this loop of warm water represents a strong bottom current from the southwest Pacific Basin which overflows the East-Pacific Ridge in the vicinity of a fracture zone. The flow within the cold-water tongue is moderate in its southwestern sections and weak in the southeast.

Bottom photographic current evidence is in agreement with the circulation pattern as found from the potential temperature and oxygen distributions. The circulation found by relating the parameter distribution to velocity field is only in relative terms. Direct current measurements are needed to determine volume transport.

THE U.S.N.S. *Eltanin* has been employed by the National Science Foundation for Antarctic oceanographic research since 1962. The physical oceanographic data were collected and processed by the Lamont Geological Observatory (FRIEDMAN, 1964; JACOBS, 1965). A total of 496 hydrographic stations was completed by the end of Cruise 20 in November, 1965. Observations have been made between 20°W and 170°W except for a four-week cruise (#16) south of New Zealand. A major part of the data is south of 55°S but during 1965 hydrographic stations were taken as far north as 45°S. This paper deals with the bottom and near-bottom water in the area shown in Fig. 1.

The influence of Antarctica on the bottom circulation of the world ocean is well known (WiJST, 1936). However, due to the paucity of data on the bottom conditions in the Antarctic oceanic area (Southern Ocean), the bottom circulation in this vicinity

♦Contribution no. 966 from the Lamont Geological Observatory.

f Lamont Geological Observatory of Columbia University, Palisades, N.Y.

is poorly known. The recent hydrographic data and the use of bottom photographs (HEEZEN and HOLLISTER, 1964) now permit the determination of the bottom circulation patterns. No direct current measurements have been made.

The distribution of bottom parameters permits a qualitative understanding of bottom water circulation and bathymetry (such as position and sill depths of passages). The most commonly used parameter is potential temperature ( $t_p$ ). This is the *in situ* temperature with the pressure component (adiabatic effect) removed (DEFANT, 1961 p. 123). The use of potential temperature eliminates the natural parallelism of the isobaths and isotherms which masks vertical movements.

Bottom potential temperatures were calculated from tables prepared by WUST (1961) from an expansion of HELLAND-HANSEN'S (1930) tables. Only observations 3000 m or deeper and within 300 m of the bottom were used. In addition the bottom-oxygen distribution was inspected. There are 382 hydrographic stations from ten ships taken between 1912 and 1965 (Fig. 1). The U.S.N.S. *Eltanin* data comprise 235 of these.

Five bottom temperatures taken by the *Eltanin* were obtained with a thermistor device ("Thermograd," GERARD, LANGSETH and EWING, 1962) which, when attached below the hydrographic cast (JACOBS, 1965), yields a continuous record of temperature and depth. The 3000-m contour is a compilation of several sources (HEEZEN and JOHNSON, 1965; HEEZEN and THARP, 1961; HERDMAN, 1948; and a U.S.S.R. ANTARCTIC CHART, 1963) and the echo soundings at the hydrographic stations. A dashed contour line is used for the East-Pacific Ridge where the topography is rough and not well known. There are also some topographic features in the Scotia Sea which are indicated by a dashed line.

The potential temperature and oxygen distributions are a synoptical representation. The success of this approach indicates that the bottom water produced each year does not vary substantially (DEACON, 1963).

#### BOTTOM POTENTIAL TEMPERATURE

The distribution of bottom potential temperature is shown in Fig. 2. A contour interval of one tenth of a degree is used with the  $\pm 0.05^\circ\text{C}$  isotherm added in the Bellingshausen Basin. There are two areas of cold water ( $<0^\circ\text{C}$ ): (1) the Weddell Sea and southern Scotia Sea and (2) the central and southwestern Bellingshausen Basin. The former displays the most extreme values. *Eltanin* Sta. 263 has the coldest bottom potential-temperature in the area covered by the chart ( $-1.31^\circ\text{C}$ ). The warmest values are over  $1.00^\circ\text{C}$ ; they are found in the vicinity of the East-Pacific Ridge north of  $55^\circ\text{S}$ .

From the  $t_p$  distribution, it appears that no broad passage deeper than 3000 m exists in the East-Pacific Ridge as shown by the 3000 m isobath. It is more likely that the bottom water over-rides the ridge particularly at latitudes between  $56^\circ\text{C}$ - $59^\circ\text{S}$  which may be topographically more suited for this process (a fracture zone). A cold tongue of water extends across the central Bellingshausen Basin. It broadens and extends northward along  $95^\circ\text{W}$ . The northward trend of the isotherms is controlled by eight stations north of  $55^\circ\text{C}$  including three *Eltanin* stations not shown in Fig. 1. These are along  $45^\circ\text{S}$  at  $90^\circ\text{W}$ ,  $95^\circ\text{W}$  and  $100^\circ\text{W}$ .

There are great variations in the magnitude of the temperature gradients. The bottom temperatures in the Southwestern Pacific Basin vary by only a few tenths of a

degree, from slightly over + 0-5°C to + 0-9°C. The **Belligshausen Basin** has moderate gradients with larger magnitudes along its periphery. The highest temperature gradients are found in the Drake Passage and northwestern Scotia Sea. Here a tongue of cold water from the Scotia Sea is separated from warmer waters to the north and west. A temperature change of half a degree in approximately fifty kilometers takes place. Whether this tongue is confined by a topographic feature in the Drake Passage or by a dynamic restraint is not known.

The bottom waters of the Scotia Sea are derived from the Weddell Sea. The controlling sill in this interaction is through the South Orkney Ridge as suggested by

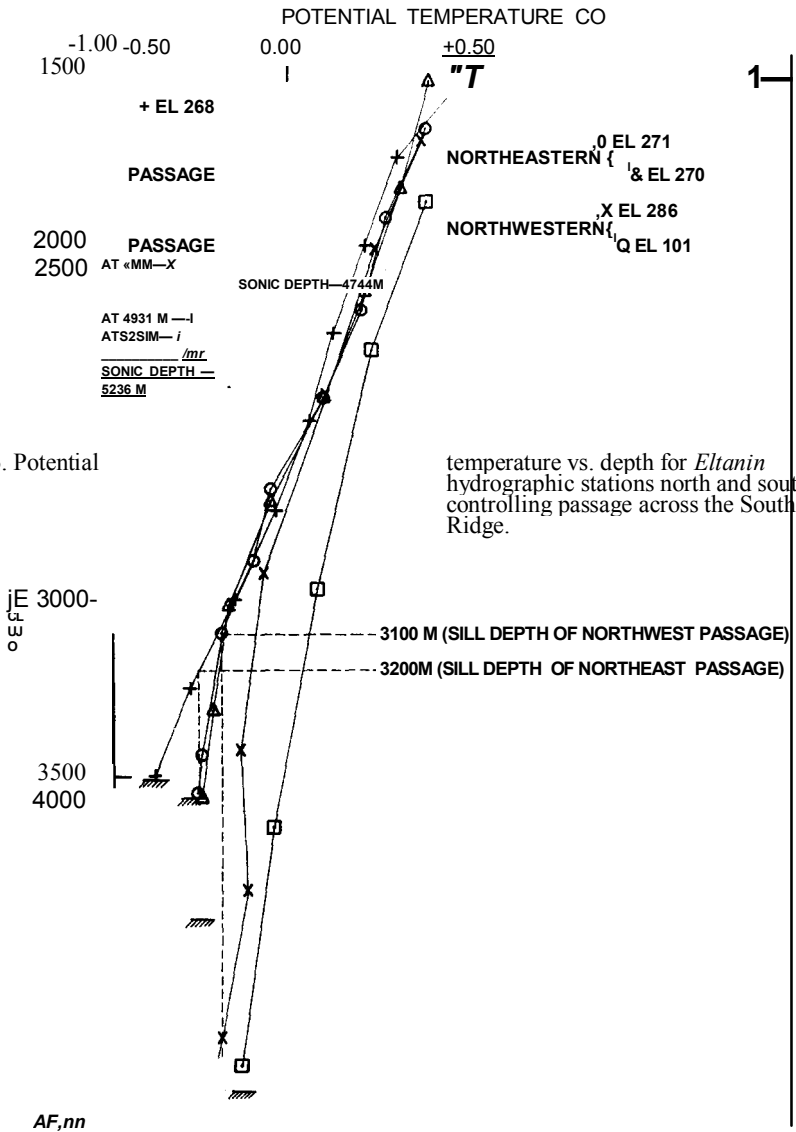


Fig. 3. Potential

temperature vs. depth for *Eltanin* hydrographic stations north and south of the controlling passage across the South Orkney Ridge.



WUST (1933). It is located at approximately 39°W. There appear to be two passages, one to the east of the topographic high (3000-m contour) and the other to the west. The sill depths of the northeastern and northwestern passage differ. Figure 3 is a potential temperature vs. depth diagram of stations north and south of the South Orkney Ridge. There are not enough data to draw a  $t_p$  profile or conclusively find the sill depth. The northeast passage has a sill depth of 3200 m while the northwest sill depth is between 3000 and 3200 m. It is probable that the deepest channel was not sampled. This would mean that the sill depth would be greater than indicated. The sill depth must be greater than 3000 m (but probably not greater than 3500 m). The passage to the east (about 31°W) is less than 3000 m.

The isotherms along the northeast and east section of the chart are controlled by the bottom potential temperature chart prepared by Wüst (1933). The isotherms directly north of the South Sandwich Trench are not drawn. They may close along the north flank of the trench or may form a tongue-like feature indicating a northward flow. The determination of the isotherm distribution would shed light on the role of the South Sandwich Trench in the transport of Antarctic Bottom Water into the Atlantic Ocean's western trough. This problem is discussed below.

The isotherms near the southern 3000-m contour of the Drake Passage are drawn so that they intersect the contour. It is possible that these isotherms remain fairly parallel to the 3000-m contour and join with the colder water in the southern Bellingshausen Basin. However, for the most part there is sufficient data to construct the isotherms with a minimum of generalization and subjective reasoning.

#### BOTTOM SALINITY

The bottom salinity values vary only slightly. In general, they are proportional to the potential temperature. The bottom salinity is lowest in the Weddell Basin (34-653‰) and reaches values of 34-720‰ in the Southwestern Pacific Basin and northern Bellingshausen Basin. The mean salinity value is 34-70‰ in the Pacific and 34-69‰ in the Atlantic. These values are representative of the bottom salinities in the entire deep Pacific which average 34-695‰ with a standard deviation of 0034‰ (WOOSTER and VOLKMANN, 1960). Since the salinity variations are slight, the distribution is not plotted.

#### BOTTOM OXYGEN

The Antarctic Bottom Water is thought to be shelf water which sinks to the bottom by vertical convection and mixing to a certain extent with the warmer deep water (DEACON, 1937; DEFANT, 1961). It is expected that the coldest bottom water would have the highest percentage of shelf water and so the highest oxygen concentration. This is shown to be true.

The oxygen distribution (Fig. 4) generally parallels the isotherms. The density of the points and the relative magnitude of the error in the oxygen determination to the observed gradients necessitate more generalized contours than those in the  $t_p$  chart. The saturation levels are fairly high, ranging from 60% to slightly over 66% of maximum oxygen concentration. The lowest temperatures have the highest percentage of saturation so the varying oxygen concentrations are not due entirely to solubility.

The oxygen concentration decreases in the direction of the flow. The amount of this decrease or deviation between the streamlines and oxygen isopleth depends on the value of the ratio of the coefficient of eddy diffusion and of the velocity, and also on the rate of consumption. Therefore, complete parallelism of the oxygen and temperature fields besides being improbable due to the accuracy of measurements is not expected since the temperature is not affected by the oxidative process. The high oxygen concentration in the bottom water creates unfavorable conditions for preservation of organic substance (RICHARDS, 1957).

Oxygen values determined by *Discovery II* are systematically 0.5 ml/l, less than those determined on *Eltanin*. After adding a factor of +0.5 ml/l, the *Discovery II* data were used as auxiliary values in drawing the contours. The *Discovery II* oxygen values are displaced on a  $t_p$ -O<sub>2</sub> plot, and in addition there is a greater scatter when compared with the *Eltanin* data (Fig. 5). It is unlikely that the difference between the *Discovery* and *Eltanin* values reflects an increase in O<sub>2</sub> over the past 20-30 years, since no corresponding oxygen difference has been noticed in the deep water of the Atlantic Ocean. Yet this deep water makes up a large percentage of the bottom water in the Southern Ocean. The other component is shelf water which is saturated with oxygen. It has been noted by WUST (1964) that "the titration of the *Discovery II* Expedition of 1931, between 50°S and 15°N have, on the average systematically given 4% lower values than the other observations." The values in the bottom waters described in this paper are about 10% too low. The discrepancy of *Discovery* oxygen data was also noted by WOOSTER and VOLKMANN, 1960.

The *Eltanin* and I.G.Y. data shown on the  $t_p$ -O<sub>2</sub> plot can be divided into sections each representing a separate geographic area. The clear separation of these areas is indicative of high gradients at their boundaries. The slope of the central line in the distribution becomes smaller at the low temperatures with an apparent discontinuity between the Weddell Basin and the northern Scotia Basin values (between areas A and B). The general relationship between the bottom potential-temperature and oxygen, shown in Fig. 5, is continued in the bottom waters of the Pacific Ocean (WOOSTER and VOLKMANN, 1960), though it is improbable that the bottom waters from the Bellingshausen Basin flood the entire Pacific Ocean.

#### BOTTOM WATER SOURCE AREAS

From the bottom distributions of potential temperature and oxygen, it is clear that the Weddell Sea is a source of extremely cold highly oxygenated bottom water. This water owing to its high density and to the topographic conditions can flow over long distances with little mixing within the overlying water. WUST (1936, 1957) has shown that the Weddell Sea water reaches northward to between 40° and 45°N in the western Atlantic, and has strong influences on the Indian and Pacific bottom circulation. There is little doubt that the Weddell Sea is a major source of bottom water and a primary hydrodynamical sink of the world oceans (STOMMEL, 1957). The lack of data in the ice-covered areas of the Weddell Sea does not permit exact location of bottom-water production, but a source at the western boundary of the Sea is inferred (DEACON, 1963).

The cold tongue of water in the southwestern and central Bellingshausen Basin comes either from the region of the Ross Sea or from the Indian Ocean. However,

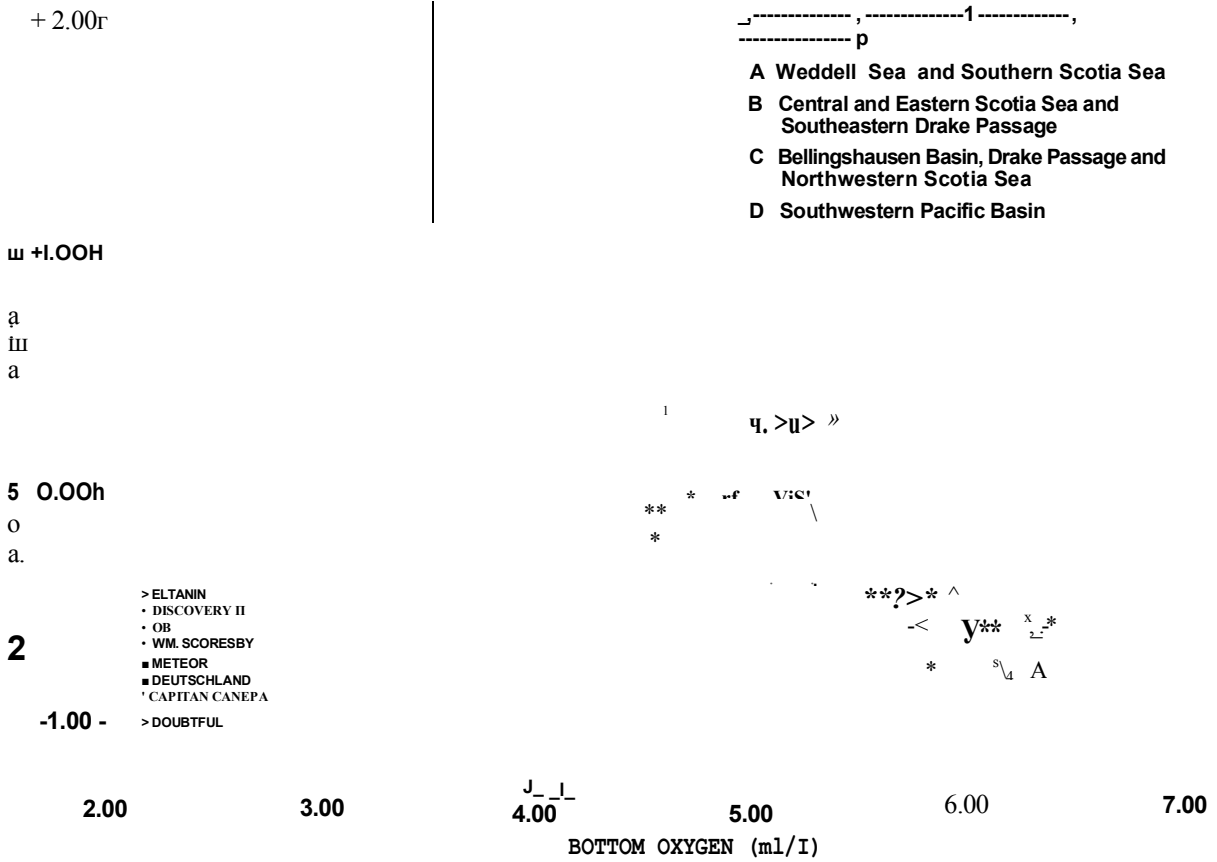


Fig. 5. Potential temperature vs. oxygen of the bottom water between 20°W and 170°W south of 50°S.

data taken by *Ob* northwest of the Ross Sea fails to support the Indian Ocean source. It appears that the Ross Sea does produce some bottom water though (as suggested by DEACON, 1937) the most dense water may be contained in deep depressions within the Ross Sea. The cold tongue is not so extreme as that of the Weddell Sea and its worldwide influence is hampered by this and by topographic restraints of the Bellingshausen Basin.

BOTTOM CIRCULATION

The true circulation cannot be found in a quantitative manner from the temperature and oxygen distributions. Flow may be either parallel or cut across the isopleths. In the steady-state condition, a balance is attained between the transport of material by eddy diffusion and the transport by advection. Since the former transport can be perpendicular to the mean current, it permits a quantum of water to change its characteristics along the path of motion, and in so doing to transverse the isopleth of the material distribution. The greater the diffusion transport compared to the advection transport, the greater the deviation between the velocity and material fields.

When both diffusion and advection processes are operative, and a material source is present, a tongue-like distribution would result. The distortion of this feature would depend on the form of the velocity field. The diffusion equation in its two-dimensional form is :

$$\frac{Ay^2}{\partial y^2} \frac{\partial M}{\partial x} = pu$$

where the *x* direction is pointed along the velocity vector whose magnitude is *u*, *Ay* is the lateral coefficient of eddy diffusion (the *Az*, or vertical term is neglected) and *M* is any material or property (as salinity, temperature, etc.). By considering a simple parallel velocity field (i.e. the *x* axis is a straight line), and a material distribution at *x* = 0 in the form of (SVERDRUP, JOHNSON and FLEMING, 1942).

$$M = M_0 + \frac{mzy}{2\pi} \cos y \tag{2}$$

The distribution of *M* in the *x-y* plane is then :

$$M = M_0 + AM \exp(-g) \cos(g) \tag{3}$$

where *h* is the distance from the center of the core to the isopleth which is parallel to the tongue axis.

It can be shown from equation (3) that these two general rules follow: (1) as the ratio (*Ay/pu*) decrease, the more parallel the isopleths of *M* and the streamlines of flow, and (2) as *Ay/pu* decreases, the material gradient of *M* increases. Therefore, the greatest deviation of the velocity and material fields is found where advection is small relative to diffusion; and when the velocities are great, the flow would be mainly parallel to the isopleths of *M*. The same rules apply when both vertical and horizontal diffusion are important.

The ratio of diffusion to advection can be calculated from the material distribution by a finite difference method to approximate the differential equation. When both vertical and lateral diffusion are important, the ratios must be solved simultaneously and two material distributions are needed. The finite difference method becomes cumbersome in this case and is subject to large errors unless the material distribution gradients are very high allowing accurate measurements of distances between isopleths. There are areas in the *t<sub>v</sub>* distribution where the gradients are large enough for calculation but in the oxygen map the generalized isopleth (due to the low gradients) cannot be used to yield reliable *Ajpu* values. In addition the oxygen is not a conservative property which would mean an

inclusion of a "rate of consumption" term, which is not known. Therefore, only ratios can be found where the two-dimensional approach is valid.

Such an area is the cold tongue in the southwestern and central Bellingshausen Basin. Lateral diffusion, due to the flat sea floor, probable is much more significant than vertical diffusion. The differential equation can be written as [according to equation (1)]:

$$\frac{A_y \partial^2 \Gamma}{p u b_y^2} - \frac{bT}{b_x} \quad (4)$$

In finite difference form: (GORDON, 1965, Chapter IV)

$$\frac{A_y}{p u} = \frac{\Delta T^2}{8 S_x} \quad (5)$$

The tongue is considered to be symmetrical. The value  $b_y$  is the separation of a particular isotherm across the tongue and  $S_x$  is the distance along the axis of the tongue with a temperature change equal to the temperature difference between that particular isotherm and the temperature at the intersection of  $b_y$  with the axis.

The value of  $A_y/pu$  found by Equation (5) in the area centered at 65°S and 134°W is  $5 \times 10^5$  cm. The value further to the east (at 67°S and 95°W) is  $1 \times 10^6$  cm. Values in the southeastern parts of the basin (at 60°S and 75°W) are extremely high, having an order of magnitude of  $10^7$  cm. Therefore, the ratio increases with distance from the Ross Sea, becoming very large at the periphery of the tongue. If the  $A_y$  value is considered fairly constant, then the velocity decreases along the tongue, becoming very small in the southeastern Bellingshausen Basin. The values of the ratio along the northern branch (along 95°W) are larger (near  $10^6$  cm). It is expected that velocities here are slightly higher than to the southeast, but are still considered to be weak. The velocities can only be discussed in relative terms, as weak, moderate or strong. A moderate current would be between 5 cm/sec and 20 cm/sec; weak and strong are then smaller or larger values, respectively.

The ratio of diffusion to advection cannot be accurately determined elsewhere on the map since the influences of topography are present and/or both vertical and lateral diffusion seem to be significant. It is possible to deduce some information of the circulation based on the two general rules discussed above.

There are basically three regions which have distinct flow patterns (Fig. 6). (1) the Weddell Sea and South Sandwich Trench, (2) the Scotia Sea and (3) the Bellingshausen Basin. The three interact at their boundaries which are either topographically or dynamically controlled.

Large gradients of  $t_p$  can result from intersection of the normal temperature structure (temperature decrease with depth) and a steep topographical slope, though the isothermal surfaces are horizontal. This would result in similar gradients of opposing sides of a topographic depression. Since this condition is not noticed in Fig. 2, the gradients are felt to be associated with sloping isothermal surfaces and currents.

#### WEDDELL SEA AND SOUTH SANDWICH TRENCH

The bottom flow in the northern Weddell Sea is toward the east. The narrowness of the tongue indicates low  $A/pu$  value, and probably a moderate to strong velocity. Whether or not all of this water enters the South Sandwich Trench is not known. A major flow of the Weddell Sea Bottom Water northward may exist to the east of the trench (WUST, 1955 and 1957). It is not clear what happens to the cold water flowing on the trench floor; it may enter the Argentine Basin, however it is more probable that

the bottom water of the Argentine Basin comes from a channel east of the trench or from a shallower level over the trench. From the low temperatures in the trench and the tongue distribution, it appears that a weak northward flow of Weddell Sea Bottom Water exists. The low  $A/pu$  value is more likely caused by the small values of mixing due to the confining boundary conditions and not necessarily due to high northward velocities.

Inspection of the bottom temperatures of three stations of *Eltanin* Cruise 22 along 40°W to the north of the Scotia Ridge indicates that the cold water penetrates westward from the trench to positions northwest to South Georgia. The warmer Pacific Bottom Water must override this denser layer.

#### SCOTIA SEA

The bottom waters of the Scotia Sea derived from the 3200-m level of the Weddell Sea have little means of escape except by vertical diffusion with the deep water. The bottom water is dense enough to prohibit the Pacific Bottom Water from penetrating into the Scotia Sea. The Pacific water is compressed into a very rapid bottom-current which leaves the Scotia Sea and enters the South Atlantic through a passage west of Shag Rocks. From the dynamic topographies of the pressure surfaces in the area, it appears that this pattern extends to shallow depths. It must supply a large quantity of Pacific water to the Atlantic Ocean (CLOWES, 1933).

The water flow within the Scotia Sea must be accomplished mostly by diffusion and only weak to moderate bottom velocities are expected. The exact nature of the potential temperature distribution and the bottom flow in the passage to the east of South Georgia is not clear. The bottom water in the trench is derived from east of the South Sandwich Islands and not from the Scotia Sea. Therefore, if the Scotia bottom water escapes it must override the colder trench waters. The flow across the main passage in the South Orkney Ridge and in the shallower passage to the east probably is strong.

The bottom flow in the western Scotia Basin is more active than in the east portion, as demonstrated by the packing of isotherms. The zone of very high temperature gradient from the central Drake Passage to the Scotia Ridge indicates a very low  $A/pu$  value and high bottom velocities approximately parallel to the isotherms. The high temperature in the gradient and to its north indicates that the flow is from the Pacific Ocean.

The tongue of Scotia Sea water in the southeastern Drake Passage confirms the presence of a bottom counter flow (a westerly directed current) in this area. However, the flow does not enter the Pacific Ocean though an extension along the 3000-m isobath may penetrate much further west. The bluntness of the tongue indicates a high diffusion rate and/or low velocity up to the boundaries. The significance and thickness of this countercurrent is discussed below.

#### BELLINGSHAUSEN BASIN

The cold water from the Ross Sea dominates the southwest and central Bellingshausen Basin. The flow in this feature (as discussed above) is probably moderate in the western and northern sections and weak in its eastern branch. Surrounding this water is a band of high temperature gradient. It is found near the East-Pacific Ridge and extends eastward to 105°W before becoming weaker and turning northward.

Another band of warm water is found along the coast of Chile and enters the Drake Passage. It is probable that this band loops to the north of the cold water tongue and connects with the warm water to the west. The central isotherm of this gradient on both sides is  $+0.5^{\circ}\text{C}$ .

The low  $A/pu$  which accompanies this band indicates (assuming normal  $A$  value) a strong ribbon-like flow along the northern flanks of the cold Ross Sea water which occupies the deeper parts of the Bellingshausen Basin. The main axis of this current is pushed up against the fracture zone through the East-Pacific Ridge west of  $105^{\circ}$ , and the South American continental slope in the east. (In both cases, the compression is consistent with the southern hemisphere Coriolis effect). The northward penetration from  $85^{\circ}\text{W}$  to  $100^{\circ}\text{W}$  indicates free access of the bottom waters to the north.

The warm-water current is derived from flow over the East-Pacific Ridge from the Southwestern Pacific Basin. The source must be from a flow along the northern flank of the East-Pacific Ridge around  $62^{\circ}\text{S}$ . A flow pattern of the type extends at least up to the temperature-maximum core layer at 400 m. A core study is in preparation by the author. A fairly rapid flow over the ridge aligned almost parallel to the crest with a component of flow into the Bellingshausen Basin must also occur.

The bottom circulation in the southwestern Pacific Basin region included in this study indicates sluggish conditions. The main flow in the basin is northward to the west of  $170^{\circ}\text{W}$  and accounts for most of the bottom waters in the Pacific Ocean (WUST, 1937; WOOSTER and VOLKMANN, 1960).

#### COUNTERCURRENT IN THE DRAKE PASSAGE

The separation of the tongue of cold Scotia Sea water in the Drake Passage from the surrounding waters must coincide with a layer of zero velocity. This layer can be used in dynamic calculations as a known reference layer. Figure 7 is a  $t_p$ - $S$  diagram, below 1000 m, of four *Eltanin* stations, which form a section approximately perpendicular to the region of high gradient. The bottom flow north of this gradient, and probably within it, is toward the east, while the flow south of the gradient is toward the west. It is apparent from the  $t_p$ - $S$  diagram that a strong north-south slope of water types exist in the Drake Passage. Below water type B the characteristics of the  $tp$ - $S$  curve change, indicating the influence of another water mass (the Scotia Sea bottom water). The separation of zero reference-layer is below 2351 m at Sta. 91. It must lie in the vicinity of the  $+0.30^{\circ}\text{C}$  isotherm since water colder than this can only be derived from the east (see the  $t_p$  distribution map). The  $t_p$  section (Fig. 7), indicates that the separation of the two current directions is approximately 800 m above the bottom in the center of the tongue.

The zero reference layer in the Drake Passage slopes steeply down toward the north, reaching the bottom about half way across the Passage. It is a boundary between two water masses, as suggested by WUST (1936). Such a sloping reference layer is an indication of active flow (WUST, 1924; NEUMANN, 1956; FOMIN, 1964). This flow pattern is consistent with the Coriolis action which would cause the eastward flow in the Drake Passage to be more concentrated on the north side and the westward flow on the south.

OSTAPOFF (1960) determined a reference layer in the Drake Passage by considering that the equivalent-barotropic system is valid. He concludes that the reference layer



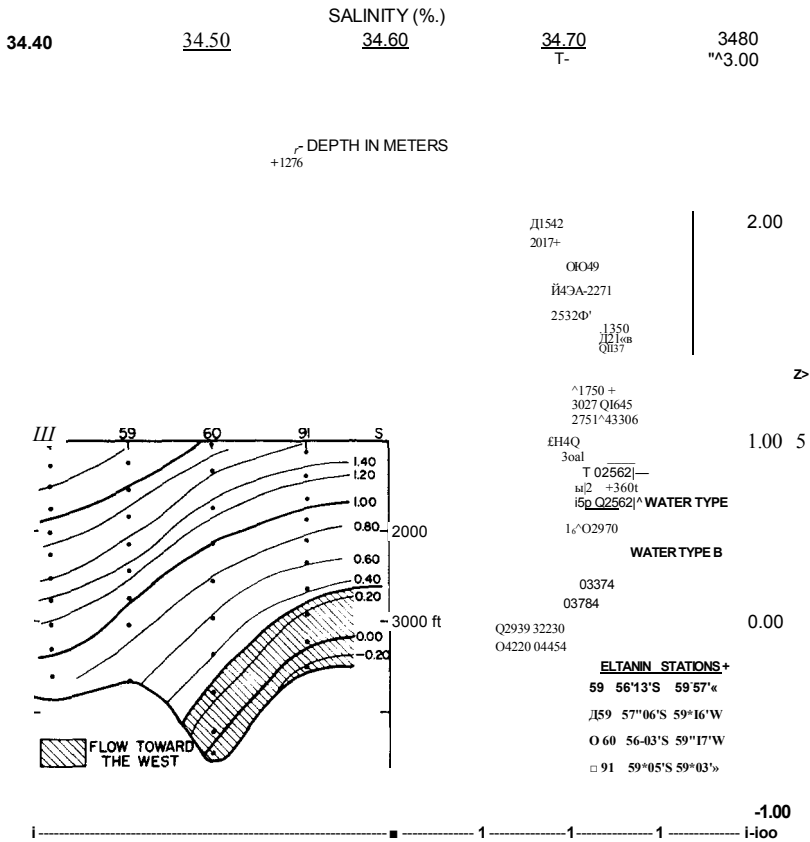


Fig. 7. Potential temperature vs. salinity and  $t_p$  section of four *Eltanin* stations along 59°W.

is inclined in the same sense as suggested in this paper. However, his reference layer is shallower, from 350 m in the south to 2500 m in the north. This implies that the westward flowing water extends across the Drake Passage. This is not supported by the bottom potential temperature distribution.

In other attempts to calculate geostrophic flow through the Drake Passage a horizontal zero-reference layer was assumed (CLOWES, 1933; KORT, 1959 and others). This assumption would lead to good results for the upper layers since these velocities are much higher than the deep velocities. However, it would give no meaningful values for the deep and bottom velocities and can lead to large discrepancies in total volume transport, as demonstrated by Clowes' value of  $110 \times 10^6 \text{ m}^3/\text{sec}$  and Ostapoff's value of  $40 \times 10^6 \text{ m}^3/\text{sec}$  for the volume transport in the Drake Passage above their chosen reference layers.

It is expected that no zero reference layer exists for zonal flow in the northern and western Drake Passage (and probably in the Bellingshausen Basin) but one can be found in the southeastern Drake Passage and most of the Scotia Sea. Further work on the dynamics of these areas is presently underway.

Numerous bottom photograph stations have been taken by U.S.N.S. *Eltanin* in the Southern Ocean. These can be used to find direct and indirect current evidence.

Currents manifest themselves on the sea floor by ripple marks (of various types), scour marks, current Hneations and by the complete absence of fine sediments exposing bare rocks or coarse residual debris (HEEZEN and HOLLISTER, 1964). Photographs displaying many animal tracks, trails, burrows, etc. indicate a lack of or very weak bottom currents. Other indirect evidence of currents is smoothing of the sea floor which partially obliterate animal evidence, and the presence of suspended matter (HOLLISTER and HEEZEN, 1966). The interpretation of the photographs are difficult in that only a limited area is viewed which may be atypical of the overall conditions of the region. This problem becomes great in regions of rough bottoms and the Precision Depth Recorder echogram must be used in conjunction with the photographs.

Photographs in the South Sandwich Trench have not revealed ripple or scour marks (HEEZEN and JOHNSON, 1965). The flow in the Trench must be a weak movement northward, as described above. It is probable that the Weddell bottom water cannot freely flow northward in the Trench for topographic reasons. The main flow of the Weddell water is to the south and east of the Trench, as shown in Fig. 6.

The bottom photographs taken in the Drake Passage have been studied by HEEZEN and HOLLISTER (1964). They conclude that " bottom currents in the northern half of the passage may reach velocities of 50 cm/sec, whereas to the south bottom currents are generally weak or absent." This is consistent with the bottom flow pattern found from the  $t_p$  map. Photographs on the South Orkney Ridge show current evidence into the Scotia Sea at the 39°W passage (HEEZEN, personal communication). It is difficult to generalize from photographic data about the bottom flow in the Scotia Sea since the bottom relief would demand more complete coverage. Photographic evidence in the northern Weddell Sea show strong currents.

The photographs in the Bellingshausen Basin were also studied by HOLLISTER and HEEZEN (1966). Ripple marks are found within the area of high temperature gradient. The flow within the tongue of cold Ross Sea water is more sluggish. The photographs show many animal traces in the southeastern region with no current evidence at all. Scour, smoothing and suspended material become more common in the western parts of this cold water feature, but there are no photographs in the southwestern Bellingshausen Basin within the main axis of the cold water. Higher velocities would be expected here. There are nodules and rocks found in the vicinity of the northern section of the cold water feature. It is not certain whether this indicates currents or low sedimentation rates or both. " However, one would in general associate at least some current with the occurrence of nodules . . . The transition from large perfect nodules to distinct current ripples in a linear west to east pattern may reflect an easterly flowing bottom current gradually restricted and thus accelerated by the Drake Passage " (HOLLISTER and HEEZEN, 1966). The  $t_v$  distribution indicates that the water in the northern Drake Passage comes from the northwest rather than from the central Bellingshausen Basin which is occupied by the colder Ross Sea water.

The photographs in the southeastern Pacific Basin show evidence of currents along crest and northern flank of the East-Pacific Ridge. They reveal little or no current evidence further north.

The bottom photographs yield strong support for the bottom pattern as found from the potential temperature distribution. There are a few discrepancies, but these may be photographs of atypical conditions, i.e. local currents due to particular topographical or dynamic controls which do not affect the large-scale  $t_v$  distribution.

*Acknowledgements*—Support for this investigation has been provided by the United States National Science Foundation through the Office of Antarctic Programs, Contract Numbers GA-194 and GA-305. I wish to thank Drs. WUST and HEEZEN for their helpful suggestions and also EDWIN WILLIAMS for his assistance.

REFERENCES

- CLOWES J. A. (1933) Influence of the Pacific on the circulation in the South-West Atlantic Ocean. *Nature, bond.*, 131, 189-191. DEACON G. E. R. (1937) The hydrology of the Southern Ocean. *Discovery Rep.*, 15, 1-124. DEACON G. E. R. (1963) The Southern Ocean. In: *The Sea*, Edited by M. N. HILL, Inter-science, New York, Vol. 2. 281-296. DEFANT A. (1961) *Physical Oceanography*, Vol. 1. Pergamon Press, 729 pp. FOMIN L. M. (1964) *The Dynamical Method in Oceanography*, Elsevier, Amsterdam, 209 pp. FRIEDMAN S. (1964) Physical Oceanographic data obtained during *Eltanin* Cruises 4, 5, and 6 in the Drake Passage, along the Chilean Coast and in the Bransfield Strait, June, 1962-January, 1963. *Lamont Geological Observatory, Tech. Rept. No. 1 GA-27* (unpublished report). GERARD R., M. LANGSETH JR. and M. EWING (1962) Thermal gradient measurements in the water and bottom sediment of the Western Atlantic. *J. geophys. Res.*, 67 (2), 785-803. GORDON A. L. (1965) Stratification and circulation in the Antillean-Caribbean basins—Quantitative study of the dynamics of the Caribbean Sea. Doctorate Thesis, Columbia University, 232 pp. HEEZEN B. C and C. D. HOLLISTER (1964) Deep-sea current evidence from abyssal sediments. *Mar. Geol.*, 1, 141-174. HEEZEN B. C and L. JOHNSON (1965) The South Sandwich Trench. *Deep-Sea Res.*, 12 (2), 185-197. HEEZEN B. C and M. THARP (1961) *The physiographic diagram of the South Atlantic, the Caribbean, the Scotia Sea and the eastern margin of the South Pacific Ocean*. Geol. Soc. Am., New York. HELLAND-HANSEN BJ, (1930) Physical oceanography and meteorology. *Rep. scient. Results Michael Sars N. Atlant. deep Sea Exped.*, 1 (2), 17 pp. HERDMAN H. F. P. (1948) Soundings taken during the *Discovery* investigations, 1932-39. *Discovery Repts.*, 25, 39-106. HOLLISTER C. D. and B. C HEEZEN (in press) The floor of the Bellingshausen Sea. In: *Deep-Sea Photography*, Edited by J. B. HERSEY, Johns Hopkins University Press. JACOBS S. (1965) Physical and chemical oceanographic observations in the Southern Oceans—U.S.N.S. *Eltanin* Cruises 7-15, 1963-64. *Lamont Geological Observatory Tech. Rept. No. 1 NSF GA-194*, (unpublished manuscript). KORT V. G. (1959) New results on the transport of Antarctic waters. *Inform. Bull. Sov. Antark. Exp.*, 9, 31-34 (In Russian). NEUMANN G. (1956) Zum problem der dynamischen Bezugsfläche insbesondere im Golfstromgebiet. *Dt. Hydrogr. Z.*, 9, 66-78. OSTAPOFF F. (1960) On the mass transport through the Drake Passage. *J. geophys. Res.*, 65 (9) 2861-2868. RICHARDS F. A. (1957) Oxygen in the ocean. *Mem. Geol. Soc. Am.*, 67 (1), 185-238. STOMMEL H. (1957) A survey of ocean current theory. *Deep-Sea Res.*, 4, 149-184. SVERDRUP H. U., M. JOHNSON and R. FLEMING (1942) In: *The Oceans*: Prentice-Hall, New Jersey, 1087 pp. USSR ANTARCTIC CHART (1963) Southern Hemisphere 1.25,000,000. Chief Administration of Geography and Cartography of the Government Geology Committee of U.S.S.R., Moscow, (in Russian). WOOSTER W. and G. VOLKMANN (1960) Indications of deep Pacific circulation from the distribution of properties at five kilometers. *J. geophys. Res.*, 65 (4), 1239-1249. WUST G. (1924) Florida und Antillenstrom eine hydrodynamische Untersuchung. *Veroff. Inst. Meeresk. Univ. Berl.*, N.F., Reihe A. H. 12, 1-8. WUST G. (1933) Das Bodenwasser und die Gliederung der atlantischen Tiefsee. *Wiss. Ergebn. Dt. atlant. Exped. 'Meteor'*, 6, 1-107. WUST G. (1936) Schichtung und Zirkulation des atlantischen Ozeans. Das Bodenwasser und die Stratosphäre. *Wiss. Ergebn. Dt. atlant. Exped. 'Meteor'*, 6 (1), 1-288. WUST G. (1937) Bodentemperatur und Bodenstrom in der pazifischen Tiefsee. *Veroff Inst. Meeresk., Univ. Berl.*, N.F. Reihe A. H. 35, 5-56.

- WUST G. (1938) Bodentemperatur und Bodenstrom in der atlantischen indischen, und pazifischen Tiefsee. *Gerlands Beitrage zur Geophysik*, 54(1), 1-8. WUST G. (1955) Stromgeschwindigkeiten im Tiefen und Bodenwasser des Atlantischen Ozeans auf Grund dynamischer Berechnung der *Meteor*. *Papers in Marine Biology and Oceanography, Supplement to Vol. 3 of Deep-Sea Res.*, 373-397. WUST G. (1957) Stromgeschwindigkeiten und Strommengen in den Tiefen des Atlantischen Ozeans. *Wiss. Ergebn. Dt. atlant. Exped. 'Meteor'*, 6, (2), 261-420. WUST G. (1961) Tables for rapid computation of potential temperature *Lamont Geological Observatory, Tech. Rept. No. 9 AT (30-1) 1808*. (unpublished report). WUST G. (1964) (with A. Gordon) Stratification and Circulation in the Antillean-Caribbean Basins. Part One—Spreading and mixing of the Water Types. *VEMA Report Series Columbia University Press*, No. 2. 201 pp.